

# Structural Asymmetry of Bacterial Reaction Centers: A $Q_y$ Resonant Raman Study of the Monomer Bacteriochlorophylls<sup>†</sup>

Dmitrij Frolov,<sup>∇</sup> Andrew Gall,<sup>‡</sup> Marc Lutz,\* and Bruno Robert

Service de Biophysique des Fonctions Membranaires, DBJC/CEA and URA 2096/CNRS, CEA-Saclay, F-91191 Gif-sur-Yvette, France

Received: August 30, 2001; In Final Form: January 7, 2002

To distinguish contributions from either of the monomer bacteriochlorophyll cofactors  $B_L$  and  $B_M$ , we have recorded Raman spectra of reaction centers (RCs) from *Rhodobacter sphaeroides*, strain R26.1 at low temperature and at resonance with the  $Q_y$  electronic band at 800 nm. Spectra excited from ferricyanide-treated RCs at 800 nm involved a single BChl species, that we identify with the  $B_L$  cofactor. Spectra excited at 810 nm in the same conditions involved participation from a second, additional cofactor, that we identify with  $B_M$ . The present, selective RR data on  $B_L$  fully confirm an earlier interpretation of difference, Soret resonant Raman spectra (Robert, B.; Lutz, M. *Biochemistry* **1988**, *27*, 5108–5114), according to which a H-bond engaged with water by the keto group of  $B_L$  should significantly strengthen upon formation of the  $P^{*+}$  radical state of the primary donor. The present data also indicate that the equivalent H-bond engaged by the keto group of  $B_M$  should strengthen as well, however by about half the enthalpy change of the L-side bond. The absolute wavenumbers, and compared  $P^{*+}$ -induced shifts of the stretching modes of the acetyl CO groups of  $B_L$  and  $B_M$  are interpreted as indicating (i) that the acetyl carbonyl of  $B_L$  is located in a higher permittivity environment than that of  $B_M$  and (ii) that the frequency of the acetyl CO vibrator of  $B_M$  may accordingly experience a stronger electric field effect from the  $P^{*+}$  radical state than that of  $B_L$ . A set of differences observed between  $B_L$  and  $B_M$  spectra specifically concerns their Mg-sensitive modes. These differences are not resulting from a differential field effect, and indicate a sizable difference of conformations between the  $MgN_4Ne_2(His)$  groups of  $B_L$  and  $B_M$ . The macroring core sizes of both  $B_L$  and  $B_M$ , however, are close to the size of relaxed, five-coordinated BChl *a* in solution. Finally, comparisons of RR spectra excited at 790, 800, and 810 nm from RCs chemically poised in the  $P^0$  or  $P^{*+}$  states revealed a sizable contribution from the neutral state of the primary donor in RR spectra excited at 810 nm only. This confirms that in electronic spectra of reduced RCs the 810 nm shoulder should arise in part from the upper excitonic component,  $P_{y+}$ , of the primary donor.

## Introduction

In photosynthetic organisms, conversion of solar energy into chemical potential energy is mediated by integral membrane proteins named reaction centers (RC). In RCs of photosynthetic purple bacteria, this energy conversion involves the reduction of a quinone molecule on the cytoplasmic side of the photosynthetic membrane and the oxidation of a cytochrome at the periplasmic surface.<sup>1</sup> From X-ray crystallographic studies,<sup>2–4</sup> the purple bacterial RC is known to consist of three membrane-spanning polypeptides, L and M, and H, two of which (L and M) assume tertiary structures related by a pseudo- $C_2$  symmetry axis. The L and M polypeptides each consists of five trans-membrane spanning helices, which together form a cage into which are bound the RC cofactors, i.e., four bacteriochlorophylls (BChl)—two of which are closely interacting and constitute the primary electron donor  $P^+$ , two bacteriopheophytins (BPheo), two quinones, one carotenoid, and one non-heme iron. The bacteriochlorin pigments and the quinones are arranged in pairs

around the pseudo- $C_2$  symmetry axis, which runs from the center of P to the non-heme iron.<sup>2,5,6</sup> As suggested by the RC structure and demonstrated by a large body of experimental data,<sup>1</sup> the light-induced electron transfer from the primary donor P sequentially involves a monomeric BChl cofactor, a BPheo, and the two quinone molecules. Despite the remarkably symmetric organization of the cofactors along the  $C_2$  axis, this electron transfer is highly asymmetric, as it essentially occurs along the set of cofactors which is more closely associated with the L subunit.<sup>7</sup> The probability for an electron to follow the L-branch pathway is thought to be at least 2 orders of magnitude higher than for the M branch.<sup>8,9</sup> This functional asymmetry of the L and M branches must essentially result from structural asymmetry between the L and M polypeptides. This structural asymmetry may influence the electron transfer directionality through several physical parameters, which have been extensively considered during the last 15 years, both from theoretical and experimental points of views. These parameters range from very local ones, such as H-bonding of a given cofactor, which may modify its redox potential and relative energies of charge-separated states,<sup>10–12</sup> to more delocalized ones, such as differences in electronic couplings between partner cofactors,<sup>13,14</sup> differences in the static electric fields, and/or differences in the dielectric constants along the L and M branches.<sup>9,15,16</sup> The functional asymmetry of the bacterial RC actually appears to

<sup>†</sup> Part of the special issue "Mitsuo Tasumi Festschrift".

\* Corresponding author. Telephone: 33 1 69 08 53 81. Fax: 33 1 69 08 43 89. E-mail: lutz@dsvidf.cea.fr.

<sup>‡</sup> Laboratoire Léon Brillouin (CEA-CNRS), CEA-Saclay, 91191 Gif-sur-Yvette, France.

<sup>∇</sup> Present address: Biophysics, Division of Physics & Astronomy, Vrije Universiteit, 1081 HV Amsterdam, Holland.

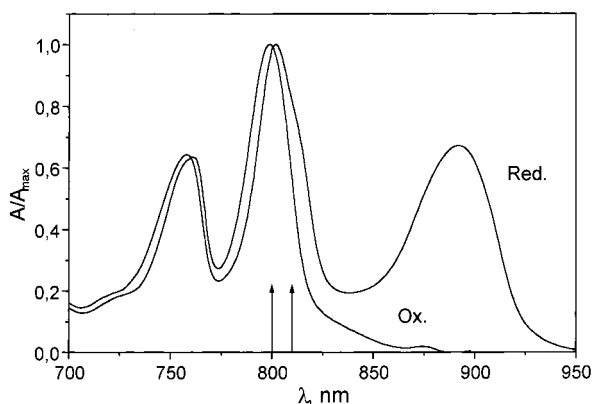


**Figure 1.** Absorption spectra of reaction centers from *Rb sphaeroides* R26.1 at 77 °K. Red.: ascorbate-treated RCs, reduced primary donor P°. Ox.: ferricyanide-treated RCs, oxidized primary donor P\*+. Arrows point at the two wavelengths, 800 and 810 nm, which have been used for exciting resonance Raman spectra.

be a multifactorial phenomenon, in which local asymmetry around the monomer BChl cofactors must play a role, possibly predominant.<sup>9,11,17</sup>

Many of the localized and delocalized environmental effects on the RC-bound bacteriochlorin cofactors can be probed by vibrational spectroscopy.<sup>18</sup> Particularly, resonance Raman spectra of BChl have been shown to contain a wealth of such information, including H-bonding states and conformations of the conjugated carbonyls,<sup>19,20</sup> coordination state of the magnesium,<sup>21,22</sup> macroring core size and conformation,<sup>22,23</sup> and local permittivity.<sup>24</sup> Information on a specific cofactor can be obtained from Raman spectra selectively excited at resonance with some specific electronic transition of this cofactor. For instance, RR spectra of the primary electron donor have been obtained selectively through preresonance with its P<sub>y</sub><sup>-</sup>, lower excitonic transition.<sup>25</sup> Differences in local environments of symmetry-related cofactors result in differences in their electronic absorption spectra. These differences can in principle be used for selectively exciting RR spectra of each of the two cofactors. Selective RR probing has so been achieved for each of the two H<sub>L</sub> and H<sub>M</sub> BPheo cofactors, using resonant excitation at each of their Q<sub>x</sub> transitions, which are distinct at low temperature,<sup>26,27</sup> as well as, more recently, using resonant excitations in the Q<sub>y</sub> band.<sup>28–30</sup>

In the bacterial RC, the Q<sub>y</sub> transitions of the monomer BChls are well separated both from those of the primary donor and BPheo cofactors (Figure 1). Moreover, there is good evidence<sup>31,32</sup> that the Q<sub>y</sub> transitions of the BCh<sub>L</sub> and BCh<sub>M</sub> cofactors are not exactly overlapping in *Rb sphaeroides* RCs, B<sub>M</sub> absorbing some 10 nm further to the red than B<sub>L</sub>. These characteristics of the Q<sub>y</sub> transitions constitute an incentive for attempting selective resonance Raman excitations of either BCh<sub>L</sub> or BCh<sub>M</sub> around 800 nm which would allow detailed comparisons of the structures and local environments of the two cofactors, in line with their possible role in the functional asymmetry of the RC.<sup>9,11,17</sup> These experiments however are very difficult because the Q<sub>y</sub> bands correspond to the lowest singlet, S<sub>1</sub> transitions of the bacteriochlorins, which are very radiative. Different attempts have been made to overcome this technical problem,<sup>33</sup> either recording the RR spectra in a classical, straightforward way<sup>30,34</sup> or using the so-called SERDS difference method.<sup>35,36</sup> Although some of the results obtained by these groups were not entirely consistent (see discussions in refs 30, 33, and 35), the data for the accessory BChls excited at or near to 800 nm appeared quite encouraging, with excellent agreement

between the more recent data obtained by the two methods, particularly in the lower frequency regions. We thus attempted careful recording of low-temperature RR spectra at full resonance with their Q<sub>y</sub> transition, with the double objective of (i), accurately recording the higher frequency regions of the spectra, which involve most of the currently identified reporter bands for the structural and environmental characteristics of BChl,<sup>37</sup> and (ii) of selectively recording RR spectra of either B<sub>L</sub> or B<sub>M</sub>, to compare their structures and environments. We here report these spectra, which represent significant improvement in terms of signal-to-noise ratios from previously published ones. At variance with previous reports<sup>30,38</sup> we show that, in the oxidized state P\*<sup>+</sup> of the primary donor, clear differences are observed between the RR spectra of B<sub>L</sub> and B<sub>M</sub>. Taken together with earlier data on RCs with reduced primary donor,<sup>20</sup> these differences allow a detailed, comparative discussion of the states of BCh<sub>L</sub> and BCh<sub>M</sub> in the *Rb sphaeroides* RCs.

## Materials and Methods

**Membrane Preparation and Protein Isolation.** The R26.1 (carotenoidless) strain of *Rhodobacter (Rb.) sphaeroides* was grown photosynthetically at 28 °C in Bose medium.<sup>39</sup> Cytoplasmic membranes were prepared and solubilized according to previously described methods.<sup>40</sup> Washed membranes were diluted to an A800 of 50 with Tris buffer (20 mM Tris·HCl, pH 8.0) then solubilized with 0.35% *N,N*-dimethyldodecylamine-*N*-oxide (LDAO) for 90 min at 26 °C followed by 3-fold dilution with Tris buffer. After high-speed centrifugation (250 Kxg, 70 min), the RC-containing supernatant was loaded onto a preequilibrated anion exchange column (20 mM Tris·HCl, pH 8.0, 0.1% LDAO, DEAE 650s, Fractogel, TosoHaas). After a salt gradient was applied (10–400 mM NaCl) the fractions were concentrated (Centriprep30, Amicon) and loaded onto a preequilibrated size exclusion column (0.075% LDAO, 50 mM NaCl, 10 mM Tris·HCl, pH 8.0 Fractogel TSK HW-55, TosoHaas). Finally, the purified RCs were subjected to a second anion exchange column (Resource Q, Pharmacia). The polypeptide composition of the RCs was verified by polyacrylamide gel electrophoresis, as described by Schagger and von Jagow.<sup>41</sup> The SDS–PAGE gels were developed using the Silver Stain Plus Kit (BioRad). For resonance Raman experiments, reaction centers samples were diluted to an OD of ca. 3 cm<sup>-1</sup>. A typical absorption spectrum at 77 K of the purified reaction centers is displayed in Figure 1.

**Spectroscopy.** Low-temperature absorption and resonance Raman spectra were recorded at 77 K from samples placed in a SMC-TBT flow cryostat (Air Liquide, Sassenage, France). Absorption spectra were recorded on a Varian Cary E5 double-beam scanning spectrophotometer. Resonance Raman spectra were obtained using a Jobin-Yvon U1000 double-monochromator Raman spectrophotometer, equipped with 600 groove/mm gratings blazed at 600 nm. Detection was performed with an N<sub>2</sub>-cooled, back-thinned, ultrasensitive, charge-coupled-device detector (Spectrum One, Jobin-Yvon, France). Excitations around 800 nm were provided by a Ti:sapphire laser (Spectra Physics, model 3900 S) pumped by an argon Coherent Innova 100 laser. Laser power reaching the sample during the recording of the Raman spectra was less than 1 mW. This corresponded, in our experimental conditions, to a flux of about 10 photons per RC per second. The reported spectra result from 1 to 50 s signal accumulations on the CCD detector. No smoothing procedure was applied to the spectra. In some of the reported spectra, luminescence backgrounds were subtracted using a standard multipoint fit procedure.

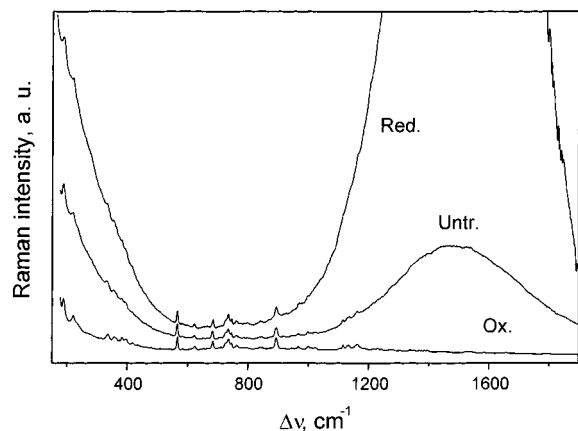


**Figure 2.** Resonance Raman spectra of RCs from *Rb. sphaeroides* R26.1 at 77 °K, excited at 800 nm. Red.: ascorbate-treated RCs; reduced primary donor. Ox.: ferricyanide-treated RCs, oxidized primary donor. Untr.: chemically untreated RCs. The proportion of photooxidized RCs contributing in the latter spectrum was 88%, as evaluated from the integrated intensity of the fluorescence band from P<sup>0</sup>, compared to that measured for the ascorbate-treated RCs.

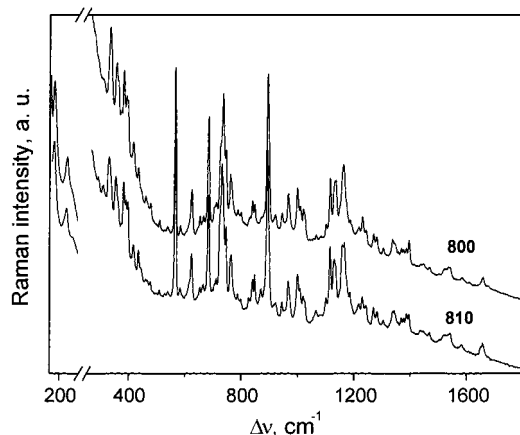


**Figure 3.** Resonance Raman spectra (150–1800 cm<sup>-1</sup> region) of ferricyanide-treated RCs from *Rb. sphaeroides* R26.1 at 77 °K. 800: 800 nm excitation. 810: 810 nm excitation.

## Results and Discussion

**Redox State of the RCs and Q<sub>y</sub> Resonant Raman Spectroscopy.** Figure 2 displays resonance Raman spectra obtained with 800 nm excitation of RC from *Rb. sphaeroides* R26.1 at 77 K in different redox conditions. When the reaction centers are poised at low redox potential prior to the Raman experiments by dithionite or ascorbate addition, a very intense fluorescence emission band is observed, which prevents the recording of the Raman signal above 1100 cm<sup>-1</sup>. The maximum of this band is located 1500 cm<sup>-1</sup> from the excitation wavelength, i.e., at 909 nm, as expected for the fluorescence of P at 77 K. This emission band disappears when the primary electron donor is fully oxidized by potassium ferricyanide. When resonance Raman spectra are recorded from chemically untreated RCs, the intensity of the 909 nm fluorescence band varies according to the power of the laser excitation beam, increasing when the laser intensity decreases. It thus may be used as a probe of the amount of reduced RCs present in the sample under recording (see Figure 2).

**Information Contents of RR Spectra Excited at 800 and 810 nm.** Figure 3 displays RR spectra obtained at 77 K from R26.1 RCs excited at 800 and 810 nm. They are very rich, with about 70 persistent, reliable features observed in the 150–1800 cm<sup>-1</sup> range. These features closely match with those previously

reported for BChl *a*<sup>18,25,37</sup> and can be confidently ascribed to this molecular species only. The present spectra recorded at 800 nm also agree well with spectra previously reported by other groups in similar experimental conditions.<sup>29,30,34,38</sup> These published spectra generally were recorded using the SERDS method, except for two spectra directly excited at 800 nm reported by Cherepy et al.<sup>38</sup> and by Eads et al.<sup>30</sup> The present spectra yield more features than the previously reported ones (Table 1). This results from significantly higher signal-to-noise ratios for our raw data, as well as probably, in part, from the visual, hence probably restrictive, selection of spectral features involved by the SERDS method. Improved signal-to-noise ratio also result in an apparently better resolution of our spectra. For instance, we resolve two components at 760 and 764 cm<sup>-1</sup> and at 840 and 848 cm<sup>-1</sup> in features observed as single bands by Eads et al.<sup>30</sup> and by Cherepy et al.<sup>38</sup> As reported in the following, this allowed us to detect and analyze differences between 810 nm-excited spectra of RCs with P either oxidized or reduced, and between spectra excited at 800 or 810 nm.

Notwithstanding the fact that they also were recorded using a direct, straightforward approach, the present spectra do not agree well with those previously reported by Palaniappan et al.<sup>42,43</sup> Similarly, it appeared difficult to reconcile the present spectra recorded from oxidized RCs with those recently acquired in the 1400–1750 cm<sup>-1</sup> range by Czarnecki et al.,<sup>44</sup> using the SERDS technique on reduced RCs. In the present spectra of reduced RCs, no band could be reliably observed above 1000 cm<sup>-1</sup>, in our experimental conditions, because of the presence of the very strong fluorescence backgrounds (Figure 2).

**Involvement of Primary Donor Contributions in RR Spectra Excited at 810 nm.** The shoulder present at 810 nm in electronic absorption spectra of RCs with a neutral primary donor (Figure 1) has been ascribed both to the upper excitonic component of the Q<sub>y</sub> transition of neutral P and to the Q<sub>y</sub> transition of the monomer BChl B<sub>M</sub>.<sup>31,45</sup> The relative participations of these two species in constituting the absorbance around 810 nm is unclear.<sup>16,32</sup> Resonance Raman spectra excited in this range may contribute to clarifying this problem if containing contributions from P (The absence of such contributions would not be conclusive, because RR intensities depend on several parameters other than species absorbance at excitation wavelength). Previous work<sup>38</sup> concluded that RR spectra of *Rb. sphaeroides* RCs excited throughout the 800 nm band did not involve any sizable contribution from P.

When comparing the RR spectra excited at 800 nm from RCs poised at low or high redox states ensuring neutral or oxidized states of the primary donor P, respectively, no significant differences indeed can be observed (Figure 4, spectra *800ox* and *800red*). However, this is not so when using 810 nm excitation. In this latter case, a limited number of small, but significant differences can be observed between reduced and oxidized centers (Figure 4, spectra *810ox* and *810red*). One of them concerns the structure of the complex band at 725–745 cm<sup>-1</sup>. In spectra of reduced RCs, this band is dominated by a 727 cm<sup>-1</sup> component which does not occur in those of oxidized centers. This feature almost exactly coincides with an intense 728 cm<sup>-1</sup> band which is characteristic of neutral P in Q<sub>y</sub> preresonance spectra excited at 1064 nm (Figure 4, spectrum *1064red*).<sup>25</sup> A 730 cm<sup>-1</sup> band also dominates the 850 nm-excited RR spectra of P published by Cherepy et al.<sup>35,47</sup> Although the strong 727 cm<sup>-1</sup> component we observe in 810 nm-excited spectra of reduced RCs is close in frequency to a 724–726 cm<sup>-1</sup> shoulder present in spectra of oxidized RC spectra, it is tempting to assign it to a specific contribution of P in the former. Yet we

**TABLE 1: Main Band Wavenumbers<sup>a</sup> Observed in RR Spectra Excited at 800 or 810 nm from Ferricyanide-Treated (P<sup>+</sup> State) and Ascorbate-Treated (P<sup>o</sup> state) Reaction Centers from *Rb Sphaeroides* R26.1 at 77 K**

800 nm oxidized	810 nm oxidized	800 nm reduced	810 nm reduced	800 nm from ref 38 <sup>b</sup>	assignment <sup>c,d</sup>
187	185	187	187	186	$\gamma$ MgN, $\tau$ (II)
221	218	220	211/219	219	$\delta$ defs
234	234	232			$\delta$ defs
265?	270				$\delta$ 2a C=O, as $\delta$ NCC, $\delta$ CCC
292	293				
312	310				$\tau$ C <sub>4a</sub> C <sub>4b</sub>
335	329/335	335	330	334	$\delta$ CNMg, $\tau$ C <sub>7a</sub> C <sub>7b</sub>
357	353	356	355	358	$\delta$ CNMg
363	363	363	364		
383	382	382	383	383	
393	391	394	392		$\tau$ C <sub>8</sub> C <sub>8a</sub> , $\nu$ MgN
398	397	398	398	398	
417	417	417		417	
435	435			436	$\delta$ CNC ?
446	445				
461	460/467			464	$\nu$ MgN, $\delta$ 9 C=O
479	477			479	
510	509			511	
538	528/538				
566	566	566	567	568	$\delta$ (III), as $\delta$ NCC( $\gamma$ )
584	584	583	584		$\delta$ 2a C=O, $\delta$ CC <sub>1</sub> C <sub>1a</sub>
624	623	624	624	624	$\delta$ C <sub>2a</sub> =O, $\gamma$ C <sub>2a</sub> =O, $\delta$ (I)
654	654				
666	664				
684	684	684	685	685	$\delta$ (IV)
705	705				$\delta$ (I)
712	711	712	710		$\delta$ defs
726	725	726	727	726	
736	731/735	732/736	730/735	736	s $\delta$ NC <sub>a</sub> C <sub>m</sub> ( $\alpha$ )
746	746	746	746	747	
761/765	760/764	760/765	759/765	765	$\delta$ (III)
787	786	787	788		$\delta$ (IV)
799	797	799			$\delta$ (IV), $\delta$ (III), $\gamma$ defs
830	825				$\gamma$ C <sub>10a</sub> =O, $\gamma$ C <sub>9</sub> =O, CH bend, $\delta$ C <sub>9</sub> =O
840	839	841			CH <sub>n</sub> bend, $\gamma$ C <sub>m</sub> H
847	847	847		843	$\delta$ defs
871	869	869			$\nu$ C <sub>8</sub> C <sub>18</sub> , CH <sub>2</sub> bend
895	892	895	890/897	894	s $\delta$ NCC <sub>m</sub> ( $\beta$ )
921	921		927	921	s $\delta$ NCC <sub>m</sub> ( $\delta$ )
944	944			945	$\delta$ defs
967	966	966/972?		967	$\nu$ C <sub>10b</sub> O, $\nu$ C <sub>10</sub> C <sub>10a</sub>
999	999	999		1000	CH <sub>3</sub> bend, $\gamma$ 2a C=O
1010	1009				CH <sub>3</sub> bend, $\nu$ CC (sat)
1020	1019			1021	CH <sub>3</sub> bend, $\nu$ CC (sat) (R6)
1026	1026				
1066	1065	1062?		1065	$\delta$ (IV), CH <sub>3</sub> bend, CH <sub>2</sub> bend
				1082	
1101	1101			1101	CH <sub>3</sub> bend, $\nu$ C <sub>7</sub> C <sub>8</sub>
1115	1115			1116	$\nu$ CN(I)
1131/1136	1129/1135			1133	CH bend, $\nu$ CN(III), $\nu$ C <sub>5</sub> C <sub>5a</sub> (R5)
1162	1158/1165	1163?		1163	$\delta$ C <sub>m</sub> H( $\beta$ ) (R4)
1186	1186			1185	CH bend, $\delta$ C <sub>m</sub> H( $\delta$ )
1217	1217				CH <sub>2</sub> bend, CH bend
1230	1229			1229	CH bend, CH <sub>2</sub> bend
1242	1242			1242	$\delta$ defs
1269	1269			1269	$\nu$ CN(IV) $\nu$ C <sub>7</sub> C <sub>17</sub>
1281	1282			1280	CH bend, CH <sub>3</sub> bend
1303	1303			1302	CH <sub>2</sub> bend, CH bend
1337	1337			1336	$\nu$ CN(III), $\delta$ C <sub>m</sub> H( $\beta$ ), CH <sub>3</sub> bend
1346	1343			1346	$\delta$ defs
1357	1357				$\nu$ CN(III), $\delta$ C <sub>m</sub> H( $\beta$ ), CH <sub>3</sub> bend
1369	1368			1369	CH <sub>3</sub> bend
1376	1376				$\delta$ C <sub>m</sub> H( $\delta$ ), CH <sub>3</sub> bend
1386	1386			1382	$\nu$ CN(I), $\delta$ C <sub>m</sub> H( $\delta$ ), CH <sub>3</sub> bend
1395	1395			1393	$\nu$ CN(I) $\delta$ C <sub>m</sub> H( $\alpha$ )
1438	1435				CH <sub>3</sub> bend, s $\nu$ C <sub>a</sub> C <sub>m</sub> ( $\beta$ ), $\nu$ CN(II)
1448	1447				CH <sub>3</sub> bend, s $\nu$ C <sub>a</sub> C <sub>m</sub> ( $\delta$ ) $\nu$ CN(IV) (R3)
1469	1468			1465	s $\nu$ C <sub>a</sub> C <sub>m</sub> ( $\alpha$ ), $\nu$ CN(II)
1500	1500				$\nu$ C <sub>b</sub> C <sub>b</sub>
1521	1519			1516	$\nu$ C <sub>b</sub> C <sub>b</sub> , s $\nu$ C <sub>a</sub> C <sub>m</sub> ( $\gamma$ ), $\nu$ CN(III)
1536/1542	1535?/1542			1534	$\nu$ C <sub>b</sub> C <sub>b</sub> , s $\nu$ C <sub>a</sub> C <sub>m</sub> ( $\gamma$ ), $\nu$ CN(III) (R2)
1585	1582			1579	as $\nu$ C <sub>a</sub> C <sub>m</sub> ( $\gamma$ ) $\delta$ )
1610	1610?				as $\nu$ C <sub>a</sub> C <sub>m</sub> ( $\alpha$ ) $\beta$ $\gamma$ ) $\delta$ ) (R1)
1658	1650/1658			1652	$\nu$ C <sub>2a</sub> =O
1677	1678			1673	$\nu$ C <sub>9</sub> =O

<sup>a</sup> Wavenumbers in cm<sup>-1</sup>. <sup>b</sup> Reference 38 (Cherepy et al. 1997): untreated RCs at 95 K. <sup>c</sup> Assignments adapted from ref 55. Abbreviations and symbols as in ref 55. Assignments of frequencies lower than 550 cm<sup>-1</sup> are tentative, due to limited accuracy of the DFT method for low frequencies, and due to the particular structure of the model BChl considered in ref 55. <sup>d</sup> (R1)...(R6): core size-sensitive bands, see ref 22.

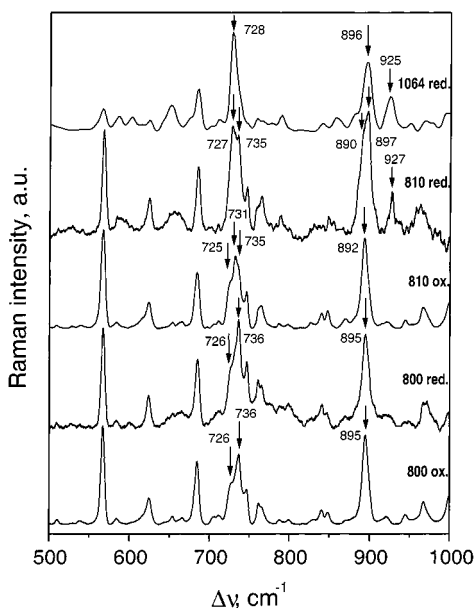


**Figure 4.** Resonance Raman spectra (500–1000  $\text{cm}^{-1}$  region) of RCs from *Rb. sphaeroides* R26.1. From bottom to top. 800 ox: ferricyanide-treated RCs at 77 °K, excited at 800 nm. 800 red: ascorbate-treated RCs at 77 °K, excited at 800 nm. 810 ox: ferricyanide-treated RCs at 77 °K, excited at 810 nm. 810 red: ascorbate-treated RCs at 77 °K, excited at 810 nm. 1064 red: ascorbate-treated RCs at room temperature, excited at 1064 nm.

are fully aware that a high relative intensity of this P band at preresonance or resonance with its lowest exciton transition in no way implies that this intensity should be also high when at resonance with the upper excitonic transition. Our interpretation is actually further supported by the observed broadening of a ca. 896  $\text{cm}^{-1}$  band in 810 nm-excited spectra of reduced RCs only (Figure 4). Again, both preresonant and resonant spectra of P excited at 1064 and 850 nm display a medium to strong band at 894–899  $\text{cm}^{-1}$ .<sup>25,35,47</sup> Two other features which are specifically present in 810 nm-excited spectra of reduced RCs may also contribute in strengthening the idea of a contribution from P. These are, i) a 211  $\text{cm}^{-1}$  shoulder on the 219  $\text{cm}^{-1}$  band (data not shown), and ii) a weak 927  $\text{cm}^{-1}$  band (Figure 4), which both match specific bands of resonant<sup>47</sup> and preresonant spectra<sup>25</sup> of P.

We thus conclude, at variance with a previous report,<sup>38</sup> that the primary electron donor in its neutral, ground-state  $\text{P}^0$  contributes in 810-nm-excited RR spectra of R26.1 *Rb. sphaeroides* RCs at 77K. The  $\text{P}^0$  species does not appear to contribute sizably in RR spectra excited at 800 nm (Figure 4, compare spectra 800red and 800ox) or at 790 nm (data not shown). The very narrow excitation spectral range in which Raman contributions from  $\text{P}^0$  are enhanced, and the coincidence of this range with the 810 nm absorption shoulder support the straightforward interpretation that these contributions originate from a resonance with the upper exciton component  $\text{P}_{y+}$  of the primary donor. More complex enhancement mechanisms are conceivable, such as resonance with vibronic sublevels of the  $\text{P}_{y-}$  transition. This specific mechanism however appears unlikely, inasmuch as it should predominantly enhance modes close to 1100  $\text{cm}^{-1}$ , rather than the set of modes ranging from 210 to 930  $\text{cm}^{-1}$  which is actually observed.

We thus take the present data as bringing confirmation that the upper exciton component  $\text{P}_{y+}$  of the primary donor in its neutral state should be involved in the 800 nm-absorbing band.<sup>31,45</sup> This involvement should not correspond to an excited-state coupling with the transitions the B cofactors<sup>48,49</sup> but, rather,

to accidental degeneracy. The  $\text{P}_{y+}$  transition should give rise, in part, to the ca. 810 nm shoulder<sup>38</sup> rather than being spread over a large spectral width.<sup>16,46</sup>

**Structural Information Available from RR Spectra Excited at 800–810 nm.** RR spectra obtained at 800 or 810 nm from ferricyanide-treated reaction centers (Figure 5) contain the whole set of bands which have been previously identified as useful in diagnosing the conformation and interaction state of protein-bound BChl *a*.<sup>18,33,37</sup>

The 800-nm-resonant spectra (Figure 5) contain two bands in the higher frequency region at 1658 and 1677  $\text{cm}^{-1}$  which may readily be assigned to the acetyl and keto carbonyl stretching modes of a BChl molecule.<sup>37</sup> According to recent high-resolution X-ray structures, (PDB Id: 1 AIJ)<sup>50</sup> (PDB Id: 1E6D),<sup>51</sup> these groups assume nearly in-plane conformations in both  $\text{B}_L$  and  $\text{B}_M$  and are indeed expected to be RR-active in these conditions. At variance with a previous report,<sup>44</sup> no bands were observed at any frequency higher than 1677  $\text{cm}^{-1}$ , ruling out any sizable activity of the ester carbonyl stretching modes expected around 1735  $\text{cm}^{-1}$ .

A very weak band is reliably observed at 1610  $\text{cm}^{-1}$ , a frequency expected for the highest methine bridge stretching mode of BChl.<sup>52</sup> This band must be sensitive to the coordination number of the magnesium via the conformation of the BChl macrocycle.<sup>21</sup> Tasumi's group has shown that several skeletal modes of chlorophyll actually are sensitive to core size.<sup>53,54</sup> Nèveke et al.<sup>22</sup> recently extended this pioneering work to BChl *a*, and identified 5 RR bands (tagged  $\text{R}_2$ – $\text{R}_6$ ), which, in addition to the 1610  $\text{cm}^{-1}$  band ( $\text{R}_1$ ), are also core-sensitive. The present 800 nm-resonant spectra also contain the whole set of  $\text{R}_2$ – $\text{R}_6$  Raman bands, at 1536, 1448, 1162, 1131/1136, and 1010/1020  $\text{cm}^{-1}$ .

Mg-sensitive modes of Bchl *a* have been identified by isotopic substitution as well as by ab initio calculations.<sup>29,37,55</sup> The present 800 nm-excited spectra display bands which may correlate with these modes, at 435, 393, 363/357, 335, and 187  $\text{cm}^{-1}$ . Previous work<sup>56</sup> has identified several RR bands of BChl *a* in the 500–800  $\text{cm}^{-1}$  range which are sensitive to the nature of the fifth Mg ligand. These bands are observed in the present 800 nm-excited spectra, in particular at 787/799  $\text{cm}^{-1}$ .

**Comparison of 800 and 810-nm-Excited RR Spectra of Oxidized RCs.** As recently discussed by King et al.,<sup>32</sup> there is good evidence that in the 800 nm electronic band, the absorption of  $\text{B}_M$  occurs at slightly lower energy than that of  $\text{B}_L$ . In the  $\text{P}^{+}$  state, a faint shoulder on the low energy side of the 800 nm band clearly present in low temperature spectra (Figure 1) should predominantly arise from  $\text{B}_M$  absorption.<sup>16,31</sup> RR spectra excited around 810 nm might thus contain higher contributions from  $\text{B}_M$  than those excited at the top of the 800 nm band or on its high-energy side. Figure 5 displays RR spectra of ferricyanide-treated R26.1 reaction centers obtained at 77 K with 800 and 810 nm excitations. The two spectra are very similar—a good indication of the high reproducibility of the present data—but they exhibit a number of significant differences, both in band frequencies and in relative intensities. The most conspicuous of these differences are listed in Table 2. Mere differences in relative intensities have not been tabulated.

**Carbonyl stretching modes of  $\text{B}_L$  and  $\text{B}_M$ .** The carbonyl stretching region (1620–1750  $\text{cm}^{-1}$ ) of the 800-nm-excited spectrum contains two bands only, at 1658 and 1677  $\text{cm}^{-1}$  (Figure 6). As discussed above, these bands can readily be ascribed to the stretching modes of the acetyl and keto carbonyls of a BChl *a* cofactor, respectively. Both these bands have narrow fwhms of 12  $\text{cm}^{-1}$ , which are those expected for their arising

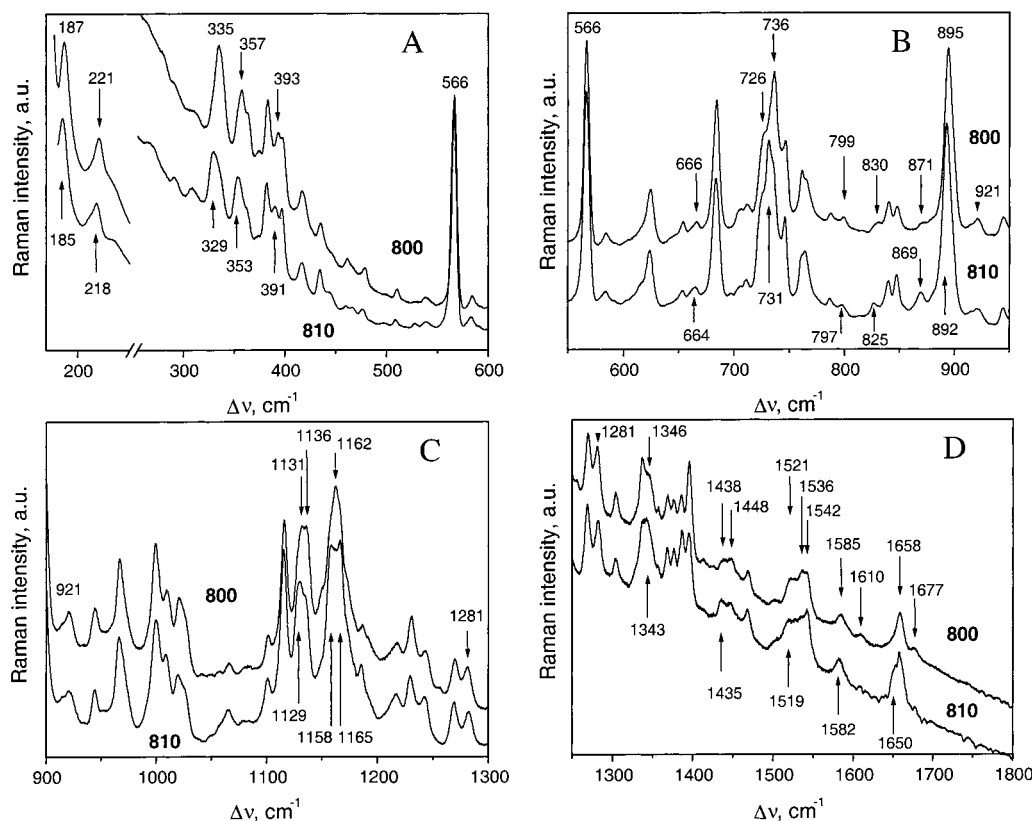


**Figure 5.** Resonance Raman spectra of ferricyanide-treated RCs from *Rb. sphaeroides* R26.1 at 77 °K excited at 800 nm (upper traces) and 810 nm (lower traces). A: 170–600  $\text{cm}^{-1}$  region, B: 550–950  $\text{cm}^{-1}$  region. C: 900–1300  $\text{cm}^{-1}$  region. D: 1250–1800  $\text{cm}^{-1}$  region.

**TABLE 2: Main Differences in Band Wavenumbers<sup>a</sup> Observed in RR Spectra Excited at 800 or 810 nm from Ferricyanide-Treated ( $\text{P}^{+\cdot}$  State) Reaction Centers of *Rb. Sphaeroides* R26.1 at 77 K**

800 nm excitation	810 nm excitation	assignment <sup>b</sup>
187	185	$\gamma$ MgN, $\tau$ (II)
221	218	$\delta$ defs
335	329/335	$\delta$ CNMg, $\tau$ C <sub>7a</sub> C <sub>7b</sub>
357	353	$\delta$ CNMg
393	391	$\tau$ C <sub>8</sub> C <sub>8a</sub> , $\nu$ MgN
736	731/735	$s$ $\delta$ NC <sub>a</sub> C <sub>m</sub> ( $\alpha$ )
799	797	$\delta$ (IV), $\delta$ (III), $\gamma$ defs
830	825	$\gamma$ C <sub>10a</sub> =O, $\gamma$ C <sub>9</sub> =O, CH bend, $\delta$ C <sub>9</sub> =O
871	869	$\delta$ defs
895	892	$s$ $\delta$ NCC <sub>m</sub> ( $\beta$ )
1131/1136	1129/1135	CH bend, $\nu$ CN(III), $\nu$ C <sub>5</sub> C <sub>5a</sub> (R5)
1162	1158/1165	$\delta$ C <sub>m</sub> H( $\beta$ ) (R4) <sup>c</sup>
1346	1343	$\delta$ defs
1438	1435	CH <sub>3</sub> bend, $s$ $\nu$ C <sub>a</sub> C <sub>m</sub> ( $\beta$ ), $\nu$ CN(II)
1521	1519	$\nu$ C <sub>b</sub> C <sub>b</sub> , $s$ $\nu$ C <sub>a</sub> C <sub>m</sub> ( $\gamma$ ), $\nu$ CN(III)
1585	1582	$as$ $\nu$ C <sub>a</sub> C <sub>m</sub> ( $\gamma\delta$ )
1658	1650/1658	$\nu$ <sub>2a</sub> C=O

<sup>a</sup> Wavenumbers in  $\text{cm}^{-1}$ . Only wavenumber differences equal to or higher than 2  $\text{cm}^{-1}$  have been included. <sup>b</sup> Assignments adapted from ref 55. Symbols and abbreviations as in ref 55. <sup>c</sup> R4: core size-sensitive band, see ref 22.

from a single population of BChl.<sup>37</sup> They accordingly should be assigned to the B<sub>L</sub> cofactor only.

These two frequencies actually match remarkably well with those, 1659 and 1675  $\text{cm}^{-1}$ , that two of us<sup>20</sup> ascribed to the carbonyl modes of B<sub>L</sub> in the  $\text{P}^{+\cdot}$  state, on the basis of a relatively complex set of difference experiments, conducted at Soret resonance, and involving the  $\text{P}^{\circ}$  and  $\text{P}^{+\cdot}$  states as well as borohydride-treated centers (Table 3). These early studies also showed that, in the  $\text{P}^{+\cdot}$  state, the stretching frequency of the

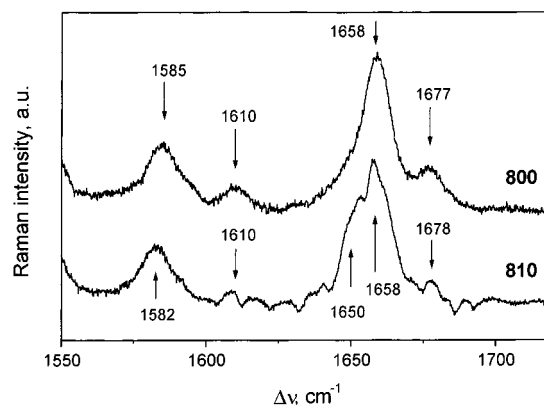


**Figure 6.** Resonance Raman spectra (1550–1720  $\text{cm}^{-1}$ ) of ferricyanide-treated RCs from *Rb. sphaeroides* R26.1 at 77 °K excited at 800 nm (upper trace) and 810 nm (lower trace). Straight base lines were subtracted from the original spectra.

**TABLE 3: Wavenumbers<sup>a</sup> of the Stretching Modes of the Acetyl and Keto Carbonyl Groups of the B<sub>L</sub> and B<sub>M</sub> Cofactors in R26.1 RCs**

	B <sub>L</sub> cofactor		B <sub>M</sub> cofactor	
	acetyl	keto	acetyl	keto
$\text{P}^{\circ b}$ state (ref 20)	1659	1689	1663	1685
$\text{P}^{+\cdot c}$ state (this work)	1658, 1659 <sup>d</sup>	1677, 1675 <sup>d</sup>	1650	1678

<sup>a</sup> Wavenumbers in  $\text{cm}^{-1}$ . <sup>b</sup>  $\text{P}^{\circ}$  state: Primary donor kept in the neutral  $\text{P}^{\circ}$  state, either by chemical reduction or low irradiance conditions (see ref 20). <sup>c</sup>  $\text{P}^{+\cdot}$  state: Primary donor chemically poised in the oxidized  $\text{P}^{+\cdot}$  radical state. <sup>d</sup> Value from ref 20.

keto group of B<sub>L</sub> was decreased by 12–14  $\text{cm}^{-1}$  from that measured at 1689  $\text{cm}^{-1}$  in the  $\text{P}^{\circ}$  state, while the stretching frequency of its acetyl group remained essentially unchanged. The present results hence fully confirm these conclusions.

The 1677/1689  $\text{cm}^{-1}$  frequencies indicate that the keto group of  $B_L$  may be engaged in a moderately strong interaction. This is consistent with this group binding a water molecule, as proposed earlier by two of us,<sup>20</sup> and as confirmed by X-ray data, which indicated its H-bonding with a water molecule located at (O–O distance) 2.7–2.8 Å from the keto oxygen.<sup>51,57</sup> The 1658/1659  $\text{cm}^{-1}$  frequency of the  $B_L$  acetyl CO is that of a free vibrator, also consistently with X-ray data, which did not indicate any suitable partner which might provide an H-bond to this group.

The spectra excited at 810 nm from RCs poised in the  $P^{*+}$  state also yield a carbonyl band at 1658  $\text{cm}^{-1}$ , consistently with a large contribution from  $B_L$  in these conditions. However, an additional feature is now apparent at 1650  $\text{cm}^{-1}$  (Figure 5). The intensity of this component, relative to that of the 1658  $\text{cm}^{-1}$  one, is maximal in spectra excited between 810 and 815 nm (data not shown). Consistently with the accepted electronic structure of the  $Q_y$  band, we assign it to a contribution from the  $B_M$  monomer BChl. A keto carbonyl band is observed at 1678  $\text{cm}^{-1}$ , a frequency which is slightly higher than that measured in 800-nm-excited spectra.

Previous work based on Soret-resonant Raman spectroscopy of borohydride-treated R26 RCs permitted Beese et al.<sup>58</sup> and Robert and Lutz<sup>20</sup> to assign a pair of carbonyl stretching frequencies observed at 1684–1685 and 1662–1663  $\text{cm}^{-1}$  in the (untreated minus treated) difference spectra, to the keto and acetyl carbonyls of  $B_M$ , respectively. The excellent agreement of the carbonyl frequencies that this study ascribed to  $B_L$  with those provided by the present results (see above) probably legitimates a quantitative comparison of the frequencies obtained for  $B_M$  in both studies. This comparison indicates that upon  $P^{*+}$  formation, the keto stretching mode of  $B_M$  should shift down by about 7  $\text{cm}^{-1}$ , while its acetyl mode should shift down by about 12  $\text{cm}^{-1}$  (Table 3).

The relative intensities of the 1658 and 1650  $\text{cm}^{-1}$  features are both rather high in the present spectra, compared to those of other bands of the 1400–1800  $\text{cm}^{-1}$  range (Figure 5). This indicates high levels of conjugation of the acetyl C=O groups with the macrorings, hence nearly in plane conformations.<sup>19</sup> This conclusion is consistent with recent high-resolution structures of *Rb sphaeroides* RCs, (PDB Id: 1 AIJ)<sup>50</sup> and (PDB Id: 1E6D),<sup>51</sup> which both involved nearly in plane conformations for the C2 acetyl groups of both  $B_L$  and  $B_M$ , but most probably not with the marked out-of-plane position proposed for the acetyl group of  $B_L$  in 2.4.1 centers published by Ermler et al. (PDB Id: 1PCR).<sup>57</sup>

From this analysis of the carbonyl stretching region, we conclude that RR spectra of oxidized RCs excited at 800 nm should essentially arise from  $B_L$  alone, while those excited in the 808–815 nm range, particularly at 810 nm, should arise from contributions from both  $B_L$  and  $B_M$ , with similar weights. Further differences between these two sets of spectra may thus be analyzed in terms of structural or environmental differences between  $B_L$  and  $B_M$ .

**Conjugated Macroring Modes.** Conformation-sensitive skeletal modes of the 1000–1600  $\text{cm}^{-1}$  region observed in the 800-nm-excited spectra occur with frequencies and band structures which are not identical to those observed for monomeric, five-coordinate BChl *a* in vitro. These differences concern the  $R_3$ – $R_6$  core-size marker bands<sup>22</sup> at 1395 (in vitro frequency: 1397  $\text{cm}^{-1}$ ), 1162 (1159/1168), 1131/1136 (1140), and 1020  $\text{cm}^{-1}$  (1017  $\text{cm}^{-1}$ ), as well as a number of other skeletal modes, such as those at 1395 (1397), 1337 (1339), 1269 (1273), 1115 (1117), and 1066 (1069) (Table 1 and ref 22). Yet, the “nominal” value

of 1610  $\text{cm}^{-1}$  observed for the  $R_1$  methine stretching mode which has highest sensitivity to core size indicates that the  $B_L$  core diameter is exactly that expected for a BChl with five-coordinated Mg in solution.<sup>22</sup> Then, the “non-nominal” values of the frequencies of the  $R_3$ – $R_6$  marker bands most probably indicate that the conjugated macrocycle of  $B_L$  is distorted from the relaxed conformation occurring in an isolated, five-coordinated BChl in solution.<sup>23</sup> The nature and amplitude of this distortion however cannot be discussed further, until a sufficient body of detailed RR data is constituted from distorted BChls for which high-resolution structures would be available.

The RR spectra excited at 810 nm yield essentially the same set of bands as those excited at 800 nm (Figure 3, Table 1). All significant differences observed between the two are indicated in Figure 5 and are listed in Table 2. Very few increases in band complexity, which should account for  $B_M$  modes being significantly distinct from  $B_L$  modes, are observed with 810 nm excitation. Only one is actually observed in the skeletal, 1000–1600  $\text{cm}^{-1}$  range, and concerns the  $R_4$  marker band. In the same range, no other of those modes which were identified above as significantly differing between  $B_L$  and BChl in vitro can actually be significantly differing between  $B_M$  and  $B_L$  (Table 2). We conclude on this basis that in R26.1 RCs, the conjugated parts of the macrocycles of the  $B_L$  and  $B_M$  cofactors must share almost the same conformation. This nearly common conformation should differ significantly from the average, relaxed one assumed by five-coordinate BChl *a* in solution.

**Mg-Sensitive Modes.** Further differences occur between 800- and 810 nm-excited spectra, mostly in the lower frequency, 200–400  $\text{cm}^{-1}$  region (Table 2). Interestingly, the frequency differences observed at 187/185, 329/335, 357/353, and 393/391  $\text{cm}^{-1}$  are likely to concern normal modes of BChl *a* which involve motions of the Mg atom.<sup>29,37,55</sup> Yet, the Mg atoms of  $B_L$  and  $B_M$  share very similar coordination states, as they each ligate a His side chain.<sup>57</sup> Differences in Mg states must be sought in details of their coordination sphere, e.g., in the 0.1 Å difference reported by Ermler et al.<sup>57</sup> between the Mg( $B_L$ )–N $\epsilon$ 2(HisL153) bond length (2.3 Å) and the Mg( $B_M$ )–N $\epsilon$ 2(HisM180) bond length (2.2 Å). The reported specific binding of the N $\delta$ 1 atom of HisL153 to a peptidic oxygen,<sup>57</sup> confirmed by the more recent structures (PDB Id: 1 AIJ)<sup>50</sup> and (PDB Id: 1E6D),<sup>51</sup> may indeed account for a difference in electronegativity between the two Mg-liganding histidines.<sup>59</sup> Also, these differences in vibrational properties may arise from different relative orientations of the His cycles with respect to the BChl macrocycle planes as well as with respect to the pyrrolic N $_1$ N $_3$  and N $_2$ N $_4$  axes. Yet, as noted above, although clearly affecting the vibrational properties of the MgN $_4$ N $\epsilon$ 2 groups, these structural differences around the Mg atoms of  $B_L$  and  $B_M$  should not imply any significant difference in macrocycle core sizes. They thus should involve differences in geometry of the MgN $_4$ N $\epsilon$ 2 group, without involving any significant difference in position of the Mg atom with respect to the macroring plane.

**Structural Asymmetry at the Level of  $B_L$  and  $B_M$  from Their Carbonyl Stretching Modes.** Altogether, the present RR spectra indicate clear, although limited structural asymmetry at the level of the conjugated parts of the  $B_L$  and  $B_M$  cofactors of R26.1 RCs poised in the  $P^{*+}$  radical state of P. Considering the information specifically provided by the conjugated carbonyl modes, this asymmetry must be analyzed in the light of our previous results on the structural changes accompanying the  $P^{\circ}$  to  $P^{*+}$  transition in R26 RCs. In their 1988 paper, Robert and Lutz<sup>20</sup> tentatively ascribed the 12  $\text{cm}^{-1}$  downshift of the keto stretching mode of  $B_L$  to a strengthening, by about 2 kcal/mol,

of an H-bond with a water molecule, resulting from local rearrangement of the L-side upon  $P^{*+}$  formation. The same explanation may be proposed for the  $6\text{ cm}^{-1}$  downshift of the keto group of  $B_M$ , which also binds a water molecule.<sup>51,57</sup> We note that this new observation of a  $P^{*+}$ -induced shift on the  $B_M$  acetyl stretching mode similar to, although about half smaller than that formerly observed for  $B_L$ , restrains the degree of L/M asymmetry that the earlier study ascribed to this molecular event.<sup>20</sup>

On the other hand, from both crystallographic data and from its stretching frequency in the  $P^0$  state, the acetyl group of  $B_M$  does not bind any ligand. We are thus left with the need for another type of explanation, which would account for both a large downshift upon  $P^{*+}$  formation and for a low wavenumber in the  $P^{*+}$  state,  $1650\text{ cm}^{-1}$ . A first possible explanation would consist of assuming a local change in polarity accompanying  $P^{*+}$  formation, resulting from motion of a nearby polar group. Tyr M 177, which is located at 7 Å from the acetyl CO of  $B_M$  (PDB Id: 1 AIJ)<sup>50</sup> might be a candidate for such a role.

A more consistent and comprehensive interpretation of our data may be found in an electric field effect from the  $P^{*+}$  state itself on the acetyl CO of  $B_M$ . We first note that, in the  $P^0$  state, the stretching frequency,  $1663\text{ cm}^{-1}$ , of the acetyl CO of  $B_M$  is  $4\text{ cm}^{-1}$  higher than that of  $B_L$  (Table 3). Both these groups being known to be free from any localized intermolecular interaction, this difference may be simply expressed in terms of a difference in dielectric constant. The acetyl CO of  $B_M$  vibrates at a frequency which is close to that observed for five-coordinated BChl *a* in low permittivity solvents.<sup>24</sup> That of  $B_L$  indicates a significantly higher permittivity. This conclusion agrees qualitatively with recent evidence produced by Steffen et al.<sup>16</sup> from Stark effect measurements, and showing a significantly higher dielectric constant along the L branch than along the M branch. These authors calculated effective dielectric constant values of 2.5 around  $B_M$  and of 9.5 around  $B_L$ . Taking their  $\epsilon$  value of 2.5 around  $B_M$ , (consistently with the  $1663\text{ cm}^{-1}$  frequency that we observe for its acetyl CO stretch) and assuming that the in-vacuo frequency of the BChl *a* acetyl CO vibrator may be  $1668\text{ cm}^{-1}$ ,<sup>19,60</sup> application of a simple Kirkwood–Bauer–Magat-type law<sup>19,24</sup> to the  $1659\text{ cm}^{-1}$  frequency yields an  $\epsilon$  of 10 around  $B_L$ , in excellent quantitative agreement with the value calculated by Steffen et al.<sup>16</sup>

Considering this difference in dielectric constants around  $B_L$  and  $B_M$  in the  $P^0$  state, the difference in sensitivity of the acetyl CO groups of  $B_L$  and  $B_M$  to  $P^{*+}$  state formation may be accounted for by a direct electric field effect from the  $P^{*+}$  radical itself. Indeed, a growing body of experimental data<sup>61–65</sup> indicates that the very high local fields occurring within proteins are able to induce large frequency shifts of polar vibrators such as carbonyls.<sup>61–63</sup> From Stark spectroscopic data on the  $Q_y$  electronic bands, Steffen et al.<sup>16</sup> have calculated  $10^8$ – $10^9\text{ V m}^{-1}$  field values at the level of the B cofactors. These values appear quite able to induce the  $12\text{ cm}^{-1}$  shift we observed for the  $B_M$  acetyl vibrator. Qualitatively, the screening effect provided by the higher dielectric constant around  $B_L$  may account for the comparatively small shift of its acetyl CO frequency upon  $P^{*+}$  formation. The present data may constitute the first reported occurrence of a vibrational Stark effect on a Raman band in a protein.

Hence, the present results bring a picture of RC asymmetry in the area of the monomer cofactors which is fully consistent with i) a sizably higher dielectric constant on the L side than on the M side, at the levels of the acetyl groups of  $B_L$  and  $B_M$ , ii) a stronger electric field effect from the  $P^{*+}$  radical state on

the conjugated, acetyl C=O vibrator of  $B_M$  than on that of  $B_L$ . Other modes of  $B_L$  and  $B_M$  may be sensitive to this difference in field effects, accounting for some of the frequency differences listed in Table 2, as well as for certain of the relative intensity differences which can be observed in Figure 5. However, most of the differences occurring between spectra excited at 800 and 810 nm from oxidized RCs (Table 2) can be found between the same spectra excited at 800 and 810 nm from reduced RCs, in the limit of the lower signal-to-noise ratios and of their smaller spectral ranges (Table 1). This is particularly true for the Mg-sensitive bands (with a possible exception for the  $185/187\text{ cm}^{-1}$  band), and indicates that these spectral differences really are of structural origin, as discussed above, rather than field-induced.

**Acknowledgment.** During the course of this study, D.F. has benefited from a European Union Training Site grant.

### Abbreviations

- BChl: bacteriochlorophyll  
 $B_L$ ,  $B_M$ : monomer bacteriochlorophyll cofactors  
 BPheo: bacteriopheophytin  
 fwhm: full width at half-maximum  
 OD: optical density  
 PDB Id: Protein Data Bank identification number  
*Rb*: *Rhodobacter*  
 RC: reaction centers  
 RR: resonance Raman

### References and Notes

- Hoff, A. J.; Deisenhofer, J. *Phys. Rep.* **1997**, *287*, 1–247.
- Deisenhofer, J.; Epp, O.; Miki, K.; Huber, R.; Michel, H. *J. Mol. Biol.* **1984**, *180*, 385–398.
- Deisenhofer, J.; Epp, O.; Sinning, I.; Michel, H. *Nature* **1985**, *318*, 618–624.
- Allen, J. P.; Feher, G.; Yeates, T. O.; Rees, D. C.; Deisenhofer, J.; Michel, H.; Huber, R. *Proc. Nat. Acad. Sci. U. S. A.* **1986**, *83*, 8589–8593.
- Deisenhofer, J.; Michel, H. *Embo J.* **1989**, *8*, 2149–2169.
- Komiya, H.; Yeates, T. O.; Rees, D. C.; Allen, J. P.; Feher, G. *Proc. Nat. Acad. Sci. U. S. A.* **1988**, *85*, 9012–9016.
- Kirmaier, C.; Holten, D.; Parson, W. W. *Biochim. Biophys. Acta* **1985**, *810*, 49–61.
- Kellogg, E. C.; Kolaczkowski, S.; Wasielewski, M. R.; Tiede, W., *Photosynth. Res.* **1989**, *22*, 47–59.
- Gunner, M. R.; Nicholls, A.; Honig, B. *J. Phys. Chem.* **1996**, *100*, 4277–4291.
- Mattioli, T. A.; Lin, X.; Allen, J. P.; Williams, J. C. *Biochemistry* **1995**, *34*, 6142–6152.
- Heller, B. A.; Holten, D.; Kirmaier, C. *Science* **1995**, *269*, 940–945.
- Kirmaier, C.; Weems, D.; Holten, D. *Biochemistry* **1999**, *38*, 11516–11530.
- Zhang, L. Y.; Friesner, R. A. *Proc. Nat. Acad. Sci. U. S. A.* **1998**, *95*, 13603–13605.
- Kolbasov, D.; Scherz, A. J. *Phys. Chem. B* **2000**, *104*, 1802–1809.
- Parson, W. W.; Chu, Z. T.; Warshel, A. *Biochim. Biophys. Acta* **1990**, *1017*, 251–272.
- Steffen, M. A.; Lao, K.; Boxer, S. G. *Science* **1994**, *264*, 810–816.
- Kirmaier, C.; He, C.; Holten, D. *Biochemistry* **2001**, *40*, 12132–12139.
- Lutz, M.; Mäntele, W. In *The Chlorophylls*; Scheer, H., Ed.; CRC Press: Boca Raton, FL, 1991; pp 855–902.
- Lutz, M.; Hoff, A. J.; Bréhamet, L. *Biochim. Biophys. Acta* **1982**, *679*, 331–341.
- Robert, B.; Lutz, M. *Biochemistry* **1988**, *27*, 5108–5114.
- Cotton, T. M.; van Duyne, R. P. *J. Am. Chem. Soc.* **1981**, *103*, 6020–6026.
- Näveke, A.; Lapouge, K.; Sturgis, J. N.; Hartwich, G.; Simonin, I.; Scheer, H.; Robert, B. *J. Raman Spectrosc.* **1997**, *28*, 599–604.
- Lapouge, K.; Näveke, A.; Gall, A.; Ivancich, A.; Seguin, J.; Scheer, H.; Sturgis, J. N.; Mattioli, T. A.; Robert, B. *Biochemistry* **1999**, *38*, 11115–11121.



- (24) Lapouge, K.; Nèveke, A.; Sturgis, J. N.; Hartwich, G.; Renaud, D.; Simonin, I.; Lutz M.; Scheer, H.; Robert, B. *J. Raman Spectrosc.* **1998**, *29*, 977–981.
- (25) Mattioli, T. A.; Hoffmann, A.; Robert, B.; Schrader, B.; Lutz, M. *Biochemistry* **1991**, *30*, 4648–4654.
- (26) Lutz, M. In *Proc. 7th International Conference on Raman Spectroscopy*; Murphy, W. F., Ed.; North-Holland: Amsterdam, 1980; pp 520–523.
- (27) Agalidis, E.; Lutz, M.; Reiss-Husson, F. *Biochim. Biophys. Acta* **1984**, *766*, 188–197.
- (28) Palaniappan, V.; Bocian, D. F. *J. Am. Chem. Soc.* **1995**, *117*, 3647–3648.
- (29) Czarniecki, K.; Diers, J. R.; Chynwat, V.; Erickson, J. P.; Frank, H. A.; Bocian, D. F. *J. Am. Chem. Soc.* **1997**, *119*, 415–426.
- (30) Eads, D. D.; Moser, C.; Blackwood, M. E.; Ching-Yao Lin, JR.; Dutton, L.; Spiro, T. G. *Biopolym. (Biospectrosc.)* **2000**, *57*, 64–76.
- (31) Breton, J. In *The Photosynthetic Bacterial Reaction Center—Structure and Dynamics*; Breton J., Vermeglio, A., Eds.; Plenum: New York, 1988; Vol. 149, pp 59–69.
- (32) King, B. A.; McAnaney, T. B.; deWinter, A.; Boxer, S. G. *J. Phys. Chem. B* **2000**, *104*, 8895–8902.
- (33) Lutz, M. *Biospectroscopy* **1995**, *1*, 313–327.
- (34) Palaniappan, V.; Schenck, C. C.; Bocian, D. F. *J. Phys. Chem.* **1995**, *99*, 17049–17058.
- (35) Cherepy, N. J.; Shreve, A. P.; Moore, L. J.; Franzen, S.; Boxer, S.; Mathies, R. A. *J. Phys. Chem.* **1994**, *98*, 6023–6029.
- (36) Czarniecki, K.; Schenck, C. C.; Bocian, D. F. *Biochemistry* **1997**, *36*, 14697–14704.
- (37) Lutz, M.; Robert, B. In *Biological Applications of Raman Spectroscopy*; Spiro, T. G., Ed.; Wiley: New York, 1988; Vol. 3, pp 347–411.
- (38) Cherepy, N. J.; Shreve, A. P.; Moore, L. J.; Boxer, S.; Mathies, R. A. *J. Phys. Chem. B* **1997**, *101*, 3250–3260.
- (39) Bose, S. K. In *Bacterial Photosynthesis*; Gest, H., Pietro, A., Vermon, L. P., Eds.; The Antioch Press: Yellow Springs, OH, 1963; pp 501–510.
- (40) Feher, G. *Photochem. Photobiol.* **1971**, *14*, 373–387.
- (41) Schägger, H.; von Jagow, G. *Anal. Biochem.* **1987**, *166*, 368–379.
- (42) Palaniappan, V.; Aldema, M. A.; Frank, H. A.; Bocian, D. F. *Biochemistry* **1992**, *31*, 11050–11058.
- (43) Palaniappan, V.; Martin, P. C.; Chynwat, V.; Frank, H. A.; Bocian, D. F. *J. Am. Chem. Soc.* **1993**, *115*, 12035–12049.
- (44) Czarniecki, K.; Kirmaier, C.; Holten, D.; Bocian, D. F. *J. Phys. Chem. A* **1999**, *103*, 2235–2246.
- (45) Xie, X.; Simon, J. D. *Biochim. Biophys. Acta* **1991**, *1057*, 131–139.
- (46) Boxer, S. G., In *Biophysical Techniques in Photosynthesis*; Ames, J., Hoff, A., Eds.; Academic Publishers: The Netherlands, 1996; Vol. 3, pp 177–189.
- (47) Cherepy, N. J.; Shreve, A. P.; Moore, L. J.; Boxer, S.; Mathies, R. A. *Biochemistry* **1997**, *36*, 8559–8566.
- (48) Parson, W. W., Scherz, A.; Warshel, A. In *Antennas and Reaction Centres of Photosynthetic Bacteria*; Michel-Beyerle, M. E., Ed.; Springer-Verlag: Berlin, 1985; pp 122–130.
- (49) Thomson, M. A.; Zerner, M. C. *J. Am. Chem. Soc.* **1991**, *113*, 8210–8215.
- (50) Stowell, M. H.; McPhillips, T. M.; Rees, D. C.; Soltis, S. M.; Abresch, E.; Feher, G. *Science* **1997**, *276*, 812–816.
- (51) Ridge, J.; P., Fyfe, P. K.; Mcauley, K. E.; Van Brederode, M. E.; Robert, B.; Van Grondelle, R.; Isaacs, N. W.; Cogdell, R. J.; Jones, M. R. *Biochem. J.* **2000**, *351*, 567–578.
- (52) Feiler, U.; Mattioli, T. A.; Katheder, I.; Scheer, H.; Lutz, M.; Robert, B. *J. Raman Spectrosc.* **1994**, *25*, 365–370.
- (53) Fujiwara, M.; Tasumi, M. *J. Phys. Chem.* **1986**, *90*, 250–255.
- (54) Fujiwara, M.; Tasumi, M. In *Advances in Spectroscopy*; Clark, R. J. H., Hester, R. E., Eds.; J. Wiley: New York, 1987; Vol. 14, pp 407–428.
- (55) Ceccarelli, M.; Lutz, M.; Marchi, M. *J. Am. Chem. Soc.* **2000**, *122*, 3532–3533.
- (56) Lutz, M.; Robert, B. *Biochim. Biophys. Acta* **1985**, *807*, 10–23.
- (57) Ermler, U.; Fritzsche, G.; Buchanan, S. K.; Michel, H. *Structure* **1994**, *2*, 926–936.
- (58) Beese, D.; Steiner, R.; Scheer, H.; Angerhofer, A.; Robert, B.; Lutz, M. *Photochem. Photobiol.* **1988**, *47*, 293–304.
- (59) Othman, S.; Richaud, P.; Vermeglio, A.; Desbois, A. *Biochemistry* **1996**, *35*, 9224–9234.
- (60) Lutz, M. in *Photosynthesis*; Akoyunoglou, G., Ed.; Balaban ISS: Philadelphia, PA, 1981; Vol. 3, pp 461–476.
- (61) Decatur, S. M.; Boxer, S. G.; *Biochem. Biophys. Res. Commun.* **1995**, *212*, 159–164.
- (62) Volk, M.; Khodolenko, Y.; Lu, H. S. M.; Googing, E. A.; DeGrado, W. F.; Hochstrasser, R. M. *J. Phys. Chem. B* **1997**, *101*, 8607–8616.
- (63) Park, E. S.; Andrews, S. S.; Hu, R. B.; Boxer, S. G. *J. Phys. Chem. B* **1999**, *103*, 9813–9817.
- (64) Park, E. S.; Thomas, M. R.; Boxer, S. G. *J. Am. Chem. Soc.* **2000**, *122*, 12297–12303.
- (65) Andrews, S. S.; Boxer, S. G. *J. Phys. Chem. A* **2000**, *104*, 11853–11863.